nature genetics

A naturally occurring epigenetic mutation in a gene encoding an SBP-box transcription factor inhibits tomato fruit ripening

Kenneth Manning[1], Mahmut Tör[1], Mervin Poole[2], Yiguo Hong[1], Andrew J Thompson[1], Graham J King[3], James J Giovannoni[4] & Graham B Seymour[2]

A major component in the regulatory network controlling fruit ripening is likely to be the gene at the tomato Colorless non-ripening (*Cnr*) locus[1,2]. The *Cnr* mutation results in colorless fruits with a substantial loss of cell-to-cell adhesion. The nature of the mutation and the identity of the *Cnr* gene were previously unknown. Using positional cloning and virus-induced gene silencing, here we demonstrate that an SBP-box (SQUAMOSA promoter binding protein–like) gene resides at the *Cnr* locus. Furthermore, the *Cnr* phenotype results from a spontaneous epigenetic change in the SBP-box promoter. The discovery that *Cnr* is an epimutation was unexpected, as very few spontaneous epimutations have been described in plants[3,4]. This study demonstrates that an SBP-box gene is critical for normal ripening and highlights the likely importance of epialleles in plant development and the generation of natural variation.

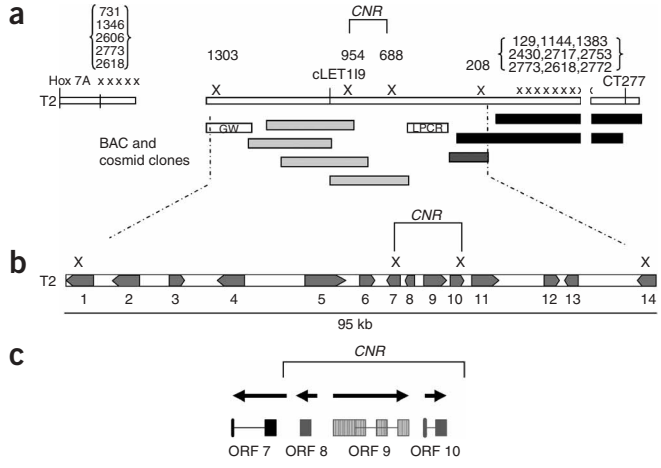

Fruits are developmental structures unique to flowering plants that are central in seed dispersal. They are also an important component of the human diet. Fleshy fruits typically become edible after they have ripened, and this process involves changes in texture, color and flavor. Substantial progress has been made in understanding the molecular and biochemical basis of these changes, including the role of ethylene in initiating and coordinating ripening in tomato (*Solanum lycopersicum*) and other climacteric fruits[5,6]. Recently, however, it has become apparent that other developmental cues are essential for ripening[7]. Progress in understanding these events has come from studies of ripening mutants of tomato such as *rin* (ripening inhibitor)[7] and *Cnr*[1,2].

The *Cnr* mutation in tomato inhibits normal ripening and produces a severe phenotype whereby fruit develop a colorless, mealy pericarp[1]. We interpret these results to mean that the gene at this locus could be central in the ripening process. This hypothesis is supported by observations of the biochemical and molecular events in *Cnr* fruits. Ripening-related pericarp carotenoid biosynthesis is absent in the mutant, with evidence for reduced ability to synthesize the carotenoid

Figure 1 High-resolution mapping of the *Cnr* locus. (**a**) The *Cnr* locus on chromosome 2 mapped in crosses between *S. lycopersicum* containing the *Cnr* mutation and *S. cheesmaniae*. The locus lies close to the cLET1I9 marker in a 13-kb interval delineated by crossovers in plants 945 and 688. The next closest crossovers on either side of the *Cnr* locus are in plants 1303 and 208. A physical contig of BAC (filled black bars) and cosmid clones (filled gray bars), a long-range PCR product (LPCR) and a series of gene walks (GW) are shown spanning the *Cnr* locus and extending to two crossovers on either side. Total physical contig is 95 kb. (**b**) Location of 14 putative ORFs in the 95-kb region spanning two crossovers on either side of the *Cnr* locus and including the 13-kb mapping interval containing the locus marked as *CNR*. (**c**) Detailed view of ORFs within the 13-kb mapping interval showing the candidate *CNR* gene ORF 7 (filled black boxes), the COPIA-like ORF 9 (cross-hatched boxes) and genes of unknown function, ORF 8 and ORF 10 (filled gray boxes).

[1]Warwick Horticulture Research International (HRI), University of Warwick, Wellesbourne, Warwick CV35 9EF, UK. [2]Plant Sciences Division, School of Biosciences, University of Nottingham, Sutton Bonington Campus, Loughborough LE12 5RD, UK. [3]Rothamsted Research, Harpenden, Hertfordshire AL5 2JQ, UK. [4]US Department of Agriculture–Agricultural Research Service and Boyce Thompson Institute for Plant Science Research, Cornell University, Tower Road, Ithaca, New York 14853-2901, USA. Correspondence should be addressed to G.B.S. (Graham.Seymour@nottingham.ac.uk).

Received 12 January; accepted 7 June; published online 9 July 2006; doi:10.1038/ng1841

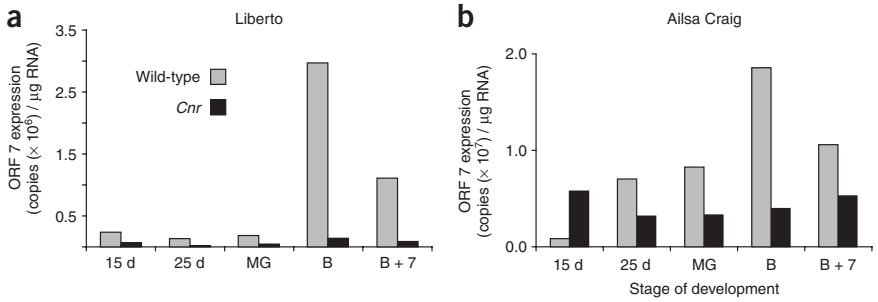

Figure 2 Expression of ORF 7 in wild-type and mutant fruits. (**a**) Expression of ORF 7 in Liberto and *Cnr* fruits, derived from a Liberto background, and (**b**) Ailsa Craig fruits and a near-isogenic line of Ailsa Craig containing the *Cnr* mutation at 15 d and 25 d post-anthesis and at mature green (MG), breaker (B) and breaker + 7 (B+7), as determined by real-time PCR.

precursor geranylgeranyl diphosphate[8]. The mealy texture of the pericarp, with its greatly reduced cell-to-cell adhesion, reflects changes in the structure of *Cnr* cell walls[2,9,10]. To place the *Cnr* gene product into a molecular framework that will help describe the ripening process, it is necessary to clone the gene. Here we report on the positional cloning and characterization of the gene at the *Cnr* locus.

In previous work, the *Cnr* locus was mapped within the euchromatin region on the long arm of tomato chromosome 2 close to the CT277 marker[11]. Using a range of markers from the tomato genetic map[12], we identified BAC and cosmid clones that we could anchor to this region. Using these clones and gene walking and long-range PCR, we generated a physical contig of 95 kb spanning the *Cnr* locus (**Fig. 1**). The 95 kb mapping interval encompassed two recombination events on either side of this locus. Sequencing the 95-kb interval uncovered 14 putative ORFs (**Fig. 1a**). The two closest crossovers flanking the *Cnr* region delineated a mapping interval of 13 kb. This interval encompassed the likely promoter region of ORF 7, predicted ORFs 8 and 9 and a possible promoter region of ORF 10 (**Fig. 1b,c**). There were no sequence differences between mutant and wild-type genomic DNA within either the 13-kb or 95-kb mapping intervals. These results indicated that a nucleotide sequence difference in the *Cnr* region was not responsible for the mutation.

We investigated the expression of genes contained within the 95 kb interval, especially those lying within the narrower 13-kb mapping interval. Semiquantitative RT-PCR demonstrated that out of 14 ORFs in the 95-kb interval, 13 were expressed in the pericarp. However, 12 of these were also expressed in leaves, and of all the ORFs in the 13-kb interval, only ORF 7 showed fruit-specific expression. ORF 7 was also the only gene that showed altered expression in mutant fruits (**Fig. 2**). Quantitative RT-PCR indicated a substantial reduction in the levels of ORF 7 transcript in the mutant during ripening. This is illustrated in **Figure 2**, where expression of ORF 7 is shown in both the original mutation derived from a Liberto background (**Fig. 2a**) and *Cnr* in a near-isogenic line in Ailsa Craig (**Fig. 2b**). We determined the expression profile of ORF 7 in a range of individual plants showing wild-type and mutant phenotypes from our mapping populations and other crosses, with consistent results (K.M. and G.B.S., unpublished data). The sequence of ORF 7 showed homology to genes of the SBP-box (*SPL*) family of transcription factors. The genetic mapping and expression data provided strong evidence that this was the gene at the *Cnr* locus. We named this gene *LeSPL-CNR*.

The absence of a nucleotide sequence difference at the *Cnr* locus indicated that the mutation might be caused by an epigenetic change in this region of the genome. Indeed, observation of occasional revertant 'ripening' sectors that have a wild-type ripening phenotype (**Fig. 3a**) is consistent with an epimutant[3]. However, these revertant sectors were rare, observed on only three individual fruits on independent plants from more than 3,000 plants grown since 1993. This indicates that the mutation is very stable, but reversible. To investigate the epigenetic basis of the mutation, we examined the methylation status of the *LeSPL-CNR* promoter region by bisulfite sequencing. We focused on a 2.4-kb region upstream of the *LeSPL-CNR* coding sequence and within the 13-kb mapping interval (**Fig. 3b**). In the *Cnr* mutant, high levels of cytosine methylation were detected in a 286-bp contiguous region 2.4 kb upstream from the first ATG of *LeSPL-CNR* (**Fig. 3a**). The DNA in both fruit and leaf tissues was always more highly methylated in this region in plants showing the *Cnr* phenotype (**Fig. 3**). For example, the percentage methylated cytosines in genomic DNA isolated from three independent ripe fruits of Ailsa Craig (control wild-type fruits) and *Cnr* (near-isogenic line in

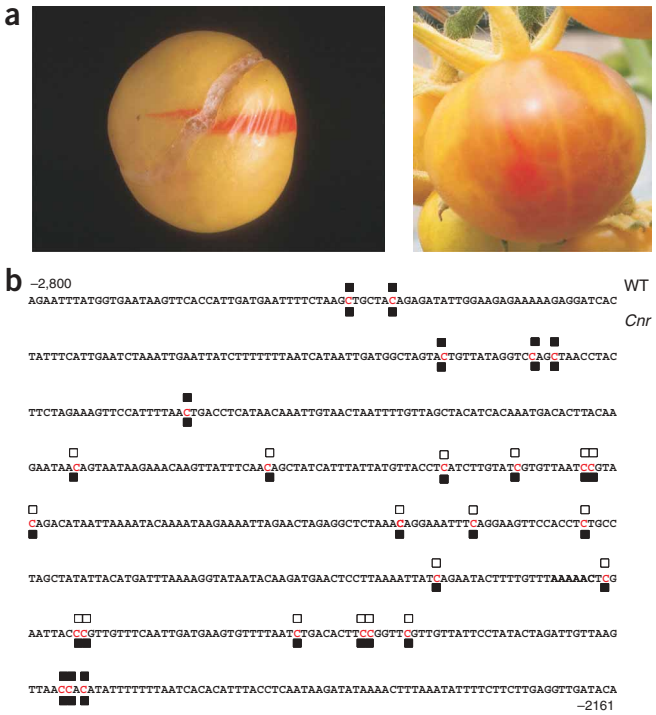

Figure 3 An epigenetic change at the *Cnr* locus. (**a**) Revertant sectors occasionally seen on mature *Cnr* fruits. (**b**) Location of methylated cytosines in DNA from wild-type (boxes above sequence) and *Cnr* (boxes below sequence) fruit in a 286-bp contiguous region upstream of the predicted ATG start codon of ORF 7, the SQUAMOSA promoter binding protein–like gene, as determined by bisulfite sequencing. Unmarked cytosines were unmethylated in both wild-type and *Cnr*. The cytosines in this region that are fully methylated in all individuals carrying the *Cnr* phenotype are shown as filled boxes; these cytosines are largely unmethylated in wild-type fruits (open boxes). Other methylated cytosine residues outside the 286-bp contiguous region showed no association with the fruit phenotype.

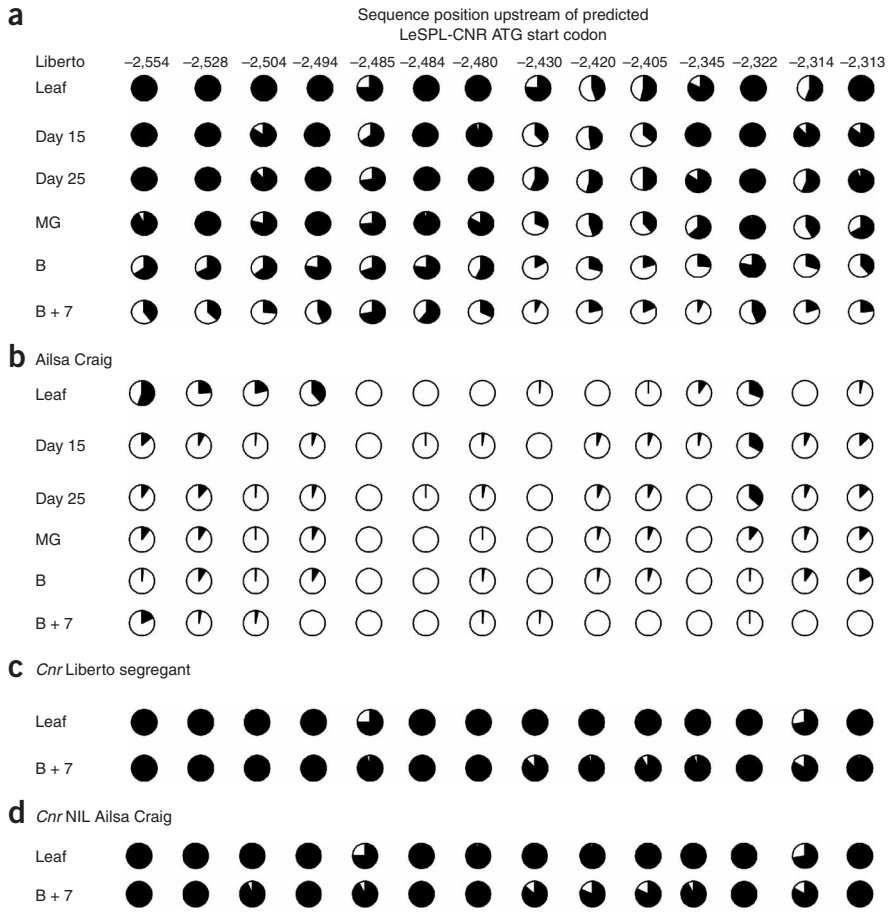

Figure 4 Percentage cytosine methylation at CpG, CpNpG and asymmetric cytosines upstream of the first ATG of ORF 7 determined by bisulfite sequencing of fruit and leaf tissues. (**a**) Wild-type Liberto. (**b**) Wild-type Ailsa Craig. (**c**) A *Cnr* segregant from the original Liberto line. (**d**) A near-isogenic line (NIL) of *Cnr* in the Ailsa Craig background. Completely filled and empty pie charts represent 100% methylated and 100% nonmethylated cytosines respectively. The pie charts represent individual determinations of percentage DNA methylation at 15 and 25 d post-anthesis and when fruit were mature green (MG), breaker (B) and breaker + 7 (B+7).

Ailsa Craig background) at 14 cytosine positions within the 286-bp region was 1.4% ± 1.4% and 86.4% ± 2.7%, respectively (± s.d.). We also found differences in overall levels of DNA methylation in this region between cultivars, with a higher percentage of methylated cytosines in the Liberto background in which the mutation arose in comparison to Ailsa Craig (**Fig. 4a**,**b**). However, the extent of cytosine methylation was always substantially greater in the mutants regardless of genetic background (**Fig. 4c**,**d**). Furthermore, the fruit tissue from the Liberto background showed a marked reduction in the percentage of cytosines that were methylated during fruit development and ripening (**Fig. 4a**). A similar trend was apparent in Ailsa Craig, although total levels of methylation were, as stated previously, much lower in this region in this genetic background (**Fig. 4b**).

Virus-induced gene silencing (VIGS) assays provided additional compelling evidence that *LeSPL-CNR* was the gene at the *Cnr* locus. We cloned the *LeSPL-CNR* gene in a potato virus X–based VIGS vector to produce PVX/*LeSPL-CNR*::GFP (**Fig. 5a**). We then injected RNA transcripts of PVX/*LeSPL-CNR*::GFP PVX/GFP recombinant viruses into the carpopodium of wild-type Ailsa Craig tomato fruit attached to the plant. We conducted experiments on fruits at various stages of development on different trusses on the same plant and on different plants. Eleven individual fruits injected with PVX/*LeSPL-CNR*::GFP produced sectors that failed to ripen normally (**Fig. 5b**). We observed that sectors eventually turned yellow and could develop a slightly pitted appearance characteristic of *Cnr* mutant fruits. All the control (PVX/GFP) fruits ripened normally (**Fig. 5c**). Real-time RT-PCR using total RNA isolated from the pericarp of the VIGS fruit (**Fig. 5**) showed that *LeSPL-CNR* expression from the green sector was ~44% of that in the surrounding ripe pericarp. This is similar to the difference in expression seen between mature green and ripe pericarp in wild-type Ailsa Craig fruits.

Our findings demonstrate that an epiallele of *LeSPL-CNR* is responsible for the *Cnr* mutation and point to an important role for the wild-type allele of *LeSPL-CNR* in normal ripening. The SBP-box family of genes are characterized by their ability to generate protein products that interact with a sequence motif in the SQUAMOSA promoter[13], but very few functional roles have been assigned to these genes. Of the SBP-box genes in *Arabidopsis thaliana*, *LeSPL-CNR* is most similar to the *SPL3* (At2g33810) gene (**Supplementary Fig. 1** online). *SPL3* may interact with promoters of the AP1 or CAL MADS-box genes of the SQUAMOSA family *in vivo* to act as a positive transcriptional regulator modulating floral development[14]. An *SPL* gene is involved in the early stages of microsporogenesis and megasporogenesis[15] and with the development of normal plant architecture[16]. Very recently, this family of genes was also associated with maize kernel development[17], a link to the development of dry fruiting structures. Our identification of an *SPL* gene at the *Cnr* locus and the presence of a MADS-box transcription factor at the *rin* locus[7] supports the model that regulatory genes involved in floral development have been recruited to new functions in modulating ripening in both dry and fleshy fruits during the course of angiosperm evolution.

The *LeSPL-CNR* protein product probably interacts with sequence motifs in the promoters of MADS-box genes of the SQUAMOSA family. This could include the ripening-related MADS-box transcription factor *TDR4*, which is a likely ortholog of the *A. thaliana* FRUITFULL (*AGL8*, also known as *FUL*) gene[2]. In *A. thaliana*, silique dehiscence is under the control of MADS-box genes *FUL* and SHATTERPROOF (*SHP*)[18].

The epigenetic allele of *LeSPL-CNR* is methylated, and hypermethylation is associated with gene silencing[19]. This change in methylation status may explain the reduced *SPL* expression in *Cnr* fruits. In plants, epigenetic states of gene expression can be inherited unchanged over many generations[3,20,21]. We speculate that the original *Cnr* mutation resulted from methylation of several normally unmethylated cytosines in the *LeSPL-CNR* promoter. These changes have been stably propagated through DNA replication, are inherited in a mendelian fashion

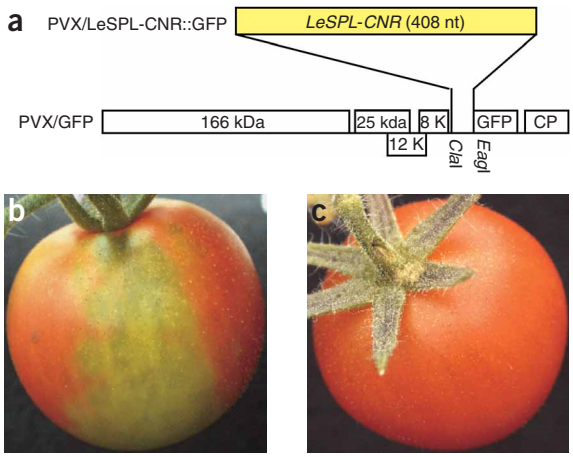

Figure 5 PVX-mediated VIGS of *LeSPL-CNR* in fruit attached to tomato plant. (**a**) Construction of VIGS vector PVX/*LeSPL-CNR*::GFP. The sequence of *LeSPL-CNR* was fused in-frame with the GFP coding sequence of PVX/GFP using the *Cla*I and *Eag*I sites. The 5′ proximal RNA-dependent RNA polymerase (166 kDa), the three viral movement proteins (25, 12 and 8 kDa ('K')) encoded by the triple-gene block and the 3′ proximal coat protein (CP) are indicated. (**b**) RNA silencing of *LeSPL-CNR* suppresses tomato ripening. Tomato fruit injected with PVX/*LeSPL-CNR*::GFP developed a non-ripening green sector. (**c**) Fruit injected with PVX/GFP was used as a negative control and showed normal ripening. Photographs were taken at 25 d post-injection of the carpopodium of young tomato fruits attached to the plants.

and result in the suppression of *LeSPL-CNR* transcription. The effect of this reduced *LeSPL-CNR* expression is to inhibit a subset of the processes involved in normal fruit development and ripening. The mutation arose in the Liberto background in which the DNA in the *LeSPL-CNR* region shows an increased propensity for methylation in comparison with that from Ailsa Craig in both leaf and fruit samples. Liberto is more similar in this respect to fruit from *S. cheesmaniae* accession LA483 (K.M. and G.B.S., unpublished). Notably, in the mutant, most of the methylated cytosines are in a symmetrical sequence context (CpG, CpNpG) believed to be maintained by MET1 and CHROMOMETHYLASE3-like methyltransferases, respectively[22].

In summary, our study of *LeSPL-CNR* demonstrates a central role for an SBP-box gene in regulating tomato fruit ripening and strengthens the argument that a substantial level of natural variation in tomato and other plant species is underwritten by epigenetic processes[23,24].

METHODS

Plant materials and growth conditions. Tomato fruits (*Solanum lycopersicum*) were grown in a heated glasshouse using standard culture practices with regular additions of N, P, K fertilizer and supplementary lighting when required. Plants were grown to three trusses. The *Cnr* mutation was detected in the F_1 hybrid cultivar Liberto[1], and a homozygous mutant line was subsequently produced after selfing for four generations. A cross was made between this *S. lycopersicum Cnr* line and *S. cheesmaniae* (LA483). The resulting F_1 was then selfed and an initial mapping population of 300 F2 progeny was generated. The F_1 was also backcrossed to *S. cheesmaniae* (LA483), and a population of 1,650 of the resulting progeny was also used in the mapping experiments. The homozygous, near-isogenic line of *Cnr* in the Ailsa Craig background was produced after five backcrosses[9].

Nucleic acid isolation. For the mapping experiments, DNA was isolated using the DNeasy kit (Qiagen). For the quantitative real-time PCR and bisulfite sequencing, total RNA and DNA were isolated simultaneously from the same tissue based on the method described in ref. 25. Total nucleic acids were precipitated from the cetyltrimethylammonium bromide (CTAB) extract with isopropanol and then cleaned up with the SSTE (1.0 M NaCl, 0.5% SDS, 10 mM Tris-HCl (pH 8.0), 1 mM EDTA (pH 8.0)) buffer before separating total RNA from DNA with 3 M LiCl.

Genetic mapping experiments. The gene at the *Cnr* locus was isolated based on genetic mapping experiments described here and in ref. 11. We used 300 F_2 and 1,650 backcross progeny from crosses between a *Solanum lycopersicum* line containing the *Cnr* mutation and *S. cheesmaniae* as the mapping populations. Individuals were scored with markers from the tomato genetic map[12] (see also Sol Genomics Network at http://www.sgn.cornell.edu/) using cleaved amplified polymorphic sequence (CAPS) and direct sequenced-based assays. A physical map of the region was then generated by hybridizing markers to tomato BAC and cosmid libraries. The BAC library was generated by Julia Vrebalov at Cornell University from *S. cheesmaniae* LA483. The *S. lycopersicum* cosmid libraries were obtained from J.J.G. at Cornell or K.M. at Warwick HRI. Gaps in the physical contig spanning the *Cnr* locus were filled by a combination of long-range PCR and gene walking as described below.

Reactions for the long PCR to bridge the gap between cosmid end sequences comprised 1 unit of Extensor High Fidelity polymerase (ABgene), 500 μM dNTPs, 200 nM of each of the primers 263H20R GSP1 and 136K18F GSP1 (**Supplementary Table 1** online) and 100 ng genomic DNA. The thermal cycling program was an initial denaturation at 92 °C for 2 min followed first by 10 cycles of 92 °C for 10 s with an extension step of 68 °C for 20 min, and second by 20 cycles of 92 °C for 10 s with an extension step of 68 °C for 20 min, extending by 20 s per cycle and ending with a 10-min extension at 68 °C. The long PCR product was digested with DNAse I in the presence of 10 mM $MnCl_2$, and fragments of 500–1,500 bp were shotgun cloned into the pSTBlue-1 vector (Novogen). Clones were sequenced using the forward and reverse vector-specific primers pSTBlue F and pSTBlue R (**Supplementary Table 1**). Any gaps in the sequence that remained between assembled contigs were closed by primer walking.

A combination of three separate methods was used for genome walking. First, we used a method using the APAgene Genome Walking kit (Bio S&T) based upon using two nested gene specific primers (GSPs) and degenerate random tagging primers. For the primary PCR, 50 ng genomic DNA was used. Second, we used a modification of the APAgene method in which the primary PCR used a GSP and a range of partially random primers adapted from the method described in ref. 26: primary reactions (15 μl) contained 500 μM dNTPs, 500 nM random primer, 200 nM of the first GSP, 0.375 units Extensor High Fidelity polymerase and 50 ng genomic DNA. The thermal cycling program was as described in the APAgene Genome Walking kit. The second PCR (15 μl) contained 500 μM dNTPs, 200 nM of nested GSP, 200 nM of the FIX primer (**Supplementary Table 1**), 0.375 units Extensor High Fidelity polymerase and 0.02 μl of the primary PCR. The thermal cycling program was 92 °C for 2 min followed by 30 cycles of 92 °C for 30 s, 57.5 °C for 30 s and 68 °C for 3 min, extending by 5 s per cycle, and ending with a 10-min extension at 68 °C. The method described in ref. 27 was modified to use ADAPTER 1 and ADAPTER 3 (**Supplementary Table 1**) based on the PCR-Select cDNA Subtraction Kit (Clontech). The long ADAPTER 1 uses the suppression PCR effect[28]. Genomic DNA was separately digested with one of the following restriction enzymes: *Dra*I, *Eco*RV, *Fsp*I, *Hpa*I, *Nru*I, *Pml*I, *Pvu*I, *Sca*I, *Stu*I, *Swa*I and *Sma*I. Reactions (15 μl) for the primary PCR comprised 200 μM dNTPs, 200 nM GSP, 200 nM PCR PRIMER 1 (**Supplementary Table 1**), 0.375 units Extensor High Fidelity polymerase and 2 or 20 ng digested genomic DNA. The thermal cycling program was 94 °C for 2 min followed by 10 cycles of 94 °C for 10 s, 68 °C for 10 min, then 20 cycles of 94 °C for 10 s, 68 °C for 10 min, extending by 10 s per cycle, and ending with a 10-min extension at 68 °C. Reactions for the second PCR were as for the primary PCR but contained a nested gene-specific primer, PCR PRIMER 2 (**Supplementary Table 1**) and 0.02 μl primary PCR. Thermal cycling was 94 °C for 2 min followed by 25 cycles of 94 °C for 10 s, 68 °C for 8 min, extending by 10 s per cycle, and ending with a 10-min extension at 68 °C.

Bisulfite sequencing. Unmethylated cytosine bases in genomic DNA were converted to uracil by sodium bisulfite using the EZ DNA Methylation Kit

(Zymo Research) according to the manufacturer's instructions. Bisulfite-converted DNA (20 ng) was then used as the template in a PCR reaction (20 µl) containing 10 µl Blue MegaMix Double PCR mixture (Microzone) and 500 nM of each primer. Forward (F) and reverse (R) primers (**Supplementary Table 2** online) for bisulfite-sequencing PCR were designed to the forward strand of the likely *LeSPL-CNR* promoter using MethPrimer software[29]. The thermal cycling program was as follows: an initial denaturation at 95 °C for 4 min 45 s followed by 38 cycles of 94 °C for 45 s, annealing for 1 min and extension at 72 °C for 30 s, ending with a 10-min extension at 72 °C. PCR products were purified by precipitation with microCLEAN (Microzone), and sequencing reactions were performed directly on the PCR products using BigDye version 3.1 DyeDeoxy Terminator Reaction Mixture (Applied Biosystems). Sequences were analyzed on a 3100 Genetic Analyzer (Applied Biosystems) capillary DNA sequencer according to the manufacturer's protocol. The peak height of cytosine (C) and thymidine (T) at various sites was measured from the electrophoretogram, and the percentage methylation (% C) calculated as $100 \times C / (C + T)$.

Analysis of gene expression. Expression of the gene at the putative ORF 7 was determined by a two-step real-time PCR method. Total RNA (1 µg) from each tissue was initially reverse transcribed using Superscript II reverse transcriptase (Invitrogen) with modifications to the manufacturer's protocol. First-strand cDNA was synthesized using a mixture of 125 ng random hexamers (Roche) and 250 ng oligo$(dT)_{12–18}$ (Amersham Biosciences) in a 20-µl reaction without added dithiothreitol. Before the addition of reverse transcriptase, the mixture was incubated at 25 °C for 2 min and then at 42 °C for 2 min. After enzyme addition, the reactions were incubated at 42 °C for 50 min and then at 25 °C for 20 min. Gene expression was analyzed by quantitative RT-PCR (QRT-PCR) using the 7900HT Fast Real-Time PCR System (Applied Biosystems). The PCR reaction (15 µl) contained 7.5 µl TAQurate 2× PCR Master Mix with SYBR Green (Epicentre), first-strand cDNA synthesized from the equivalent of 5 ng total RNA and 200 nM of each of the QRT-PCR forward and reverse primers (**Supplementary Table 1**). The QRT-PCR reverse primer spanned an intron junction and prevented any detectable amplification from genomic DNA (up to 50 ng). Absolute standards were prepared from the plasmid cLEG28P18 (TIGR Tomato Gene Index) containing the EST for ORF 7. After an initial denaturation of 95 °C for 1 min 30 s, the thermal cycling program was as follows: 40 cycles of 95 °C for 30 s, annealing at 60 °C for 30 s and extension at 72 °C for 30 s. Three technical replicates were run for each of the standards and the unknowns. The C_t value for each QRT-PCR was determined and a standard curve used to calculate absolute amounts of target cDNA. Results were expressed as the number of transcript copies per microgram total RNA.

Virus-induced gene silencing (VIGS) assay. The nucleotide sequence of *LeSPL-CNR* was PCR amplified using *Pfu* DNA polymerase (Promega) and primers pp298 and pp300 (**Supplementary Table 1**), digested with *Cla*I and *Eag*I, and cloned in-frame to the coding sequence of green fluorescence protein (GFP) in the *Cla*I/*Eag*I sites of PVX/GFP[30] to produce a VIGS vector, PVX/*LeSPL-CNR*::GFP (**Fig. 5a**). We injected RNA transcripts produced by *in vitro* transcription of PVX/*LeSPL-CNR*::GFP and PVX/GFP after linearization with *Spe*I by needle into the carpopodium of young tomato fruits (*Solanum lycopersicum* cultivar Ailsa Craig) attached to the plant[30].

Accession codes. The GenBank accession number for the 95-kb mapping interval containing *LeSPL-CNR* is DQ672601.

Note: Supplementary information is available on the Nature Genetics website.

ACKNOWLEDGMENTS

We would like to thank P. Meyer and P. Walley for useful discussions, S. Butcher and J. Abbott for assistance with annotation of the tomato genomic sequences, D. Baulcombe for providing the original PVX vector, and the Biotechnology and Biological Sciences Research Council (UK) for financial support.

AUTHOR CONTRIBUTIONS

K.M. performed research, designed experiments and wrote the paper; M.T. performed research and designed experiments; M.P. performed research; Y.H. designed and performed VIGS experiments and wrote the paper; A.J.T. performed research and designed experiments; G.K. designed experiments; J.J.G. designed experiments and wrote the paper; and G.B.S. initiated the project, designed experiments and wrote the paper.

COMPETING INTERESTS STATEMENT

The authors declare that they have no competing financial interests.

Published online at http://www.nature.com/naturegenetics
Reprints and permissions information is available online at http://npg.nature.com/reprintsandpermissions/

1. Thompson, A.J. *et al.* Molecular and genetic characterisation of a novel pleiotropic tomato-ripening mutant. *Plant Physiol.* **120**, 383–389 (1999).
2. Eriksson, E.M. *et al.* Effect of the Colourless non-ripening mutation on cell wall biochemistry and gene expression during tomato fruit development and ripening. *Plant Physiol.* **136**, 4184–4197 (2004).
3. Cubas, P., Vincent, C. & Coen, E. An epigenetic mutation responsible for natural variation in floral symmetry. *Nature* **401**, 157–161 (1999).
4. Kalisz, S. & Purugganan, M.D. Epialleles via DNA methylation: consequences for plant evolution. *Trends Ecol. Evol.* **19**, 309–314 (2004).
5. Alexander, L. & Grierson, D. Ethylene biosynthesis and action in tomato: a model for climacteric fruit ripening. *J. Exp. Bot.* **53**, 2039–2055 (2002).
6. Giovannoni, J.J. Genetic regulation of fruit development and ripening. *Plant Cell* **16**, S170–S180 (2004).
7. Vrebalov, J. *et al.* A MADS-box gene necessary for ripening at the tomato *ripening-inhibitor* (*rin*) locus. *Science* **296**, 343–346 (2002).
8. Fraser, P., Bramley, P. & Seymour, G.B. Effect of the *Cnr* mutation on carotenoid formation during tomato fruit ripening. *Phytochemistry* **58**, 75–79 (2001).
9. Orfila, C. *et al.* Altered middle lamella homogalacturonan and disrupted deposition of (1→5)-alpha-L-arabinan in the pericarp of *Cnr*, a ripening mutant of tomato. *Plant Physiol.* **126**, 210–221 (2001).
10. Orfila, C. *et al.* Altered cell wall disassembly during ripening of *Cnr* tomato fruit: implications for cell adhesion and fruit softening. *Planta* **215**, 440–447 (2002).
11. Tor, M. *et al.* Genetic analysis and FISH mapping of the Colourless non-ripening locus of tomato. *Theor. Appl. Genet.* **104**, 165–170 (2002).
12. Tanksley, S.D. *et al.* High density molecular linkage maps of the tomato and potato genomes. *Genetics* **132**, 1141–1160 (1992).
13. Klein, J., Saedler, H. & Huijser, P. A new family of DNA binding proteins includes putative transcriptional regulators of the *Antirrhinum majus* floral meristem identity gene SQUAMOSA. *Mol. Gen. Genet.* **250**, 7–16 (1996).
14. Cardon, G.H., Hohmann, S., Nettesheim, K., Saedler, H. & Huijser, P. Functional analysis of the *Arabidopsis thaliana* SBP-box gene *SPL3*: a novel gene involved in the floral transition. *Plant J.* **12**, 367–377 (1997).
15. Unte, U.S. *et al.* SPL8, an SBP-box gene that affects pollen sac development in *Arabidopsis*. *Plant Cell* **15**, 1009–1019 (2003).
16. Stone, J.M., Liang, X., Nekl, E.R. & Stiers, J.J. *Arabidopsis* AtSPL14, a plant-specific SBP-domain transcription factor, participates in plant development and sensitivity to fumonisin B1. *Plant J.* **41**, 744–754 (2005).
17. Wang, H. *et al.* The origin of the naked grains of maize. *Nature* **436**, 714–719 (2005).
18. Liljegren, S.J. *et al.* Control of fruit patterning in *Arabidopsis* by INDEHISCENT. *Cell* **116**, 843–853 (2004).
19. Martienssen, R. & Colot, V. DNA methylation and epigenetic inheritance in plants and filamentous fungi. *Science* **293**, 1070–1074 (2001).
20. Jacobson, S.E. & Meyerowitz, E.M. Hypermethylated SUPERMAN epigenetic alleles in *Arabidopsis*. *Science* **277**, 1100–1103 (1997).
21. Kinoshita, T. *et al.* One-way control of FWA imprinting in *Arabidopsis* endosperm by DNA methylation. *Science* **303**, 521–523 (2004).
22. Lindroth, A.M., Cao, X., Jackson, J.P., Zilberman, D., McCallum, C.M., Henikoff, S. & Jacobsen, S.E. Requirement of CHROMOMETHYLASE3 for maintenance of CpXpG methylation. *Science* **292**, 2077–2080 (2001).
23. Messeguer, R., Ganal, M.W., Steffens, J.C. & Tanksley, S.D. Characterization of the level, target sites and inheritance of cytosine methylation in tomato nuclear DNA. *Plant Mol. Biol.* **16**, 753–770 (1991).
24. Rapp, R.A. & Wendel, J.F. Epigenetics and plant evolution. *New Phytol.* **168**, 81–91 (2005).
25. Chang, S., Puryear, J. & Cairney, J. A simple and efficient method for isolating RNA from pine trees. *Plant Mol. Biol. Rep.* **11**, 113–116 (1993).
26. Zou, N., Ditty, S., Li, B. & Lo, S. Random priming PCR strategy to amplify and clone trace amounts of DNA. *Biotechniques* **35**, 758–760 (2003).
27. Zhang, Z. & Gurr, S. Walking into the unknown: a 'step down' PCR-based technique leading to the direct sequence analysis of flanking genomic DNA. *Gene* **253**, 145–150 (2000).
28. Diatchenko, L. *et al.* Suppression subtractive hybridization: A method for generating differentially regulated or tissue-specific cDNA probes and libraries. *Proc. Natl. Acad. Sci. USA* **93**, 6025–6030 (1996).
29. Li, L. & Dahiya, R. MethPrimer: designing primers for methylation PCRs. *Bioinformatics* **18**, 1427–1431 (2002).
30. Van Wezel, R., Liu, H., Tien, P., Stanley, J. & Hong, Y. Gene C2 of the monopartite geminivirus tomato yellow leaf curl virus-China encodes a pathogenicity determinant that is localized in the nucleus. *Mol. Plant Microbe Interact.* **14**, 1125–1128 (2001).